Mineralium Deposita (2018) 53:909–918
https://doi.org/10.1007/s00126-018-0837-x

LETTER

Carlin-style gold deposits, Youjiang Basin, China: tectono-thermal and structural analogues of the Carlin-type gold deposits, Nevada, USA

Qingfei Wang [1] · David Groves [1,2]

Received: 27 March 2018 / Accepted: 19 August 2018 / Published online: 28 August 2018

Abstract

The Triassic gold deposits of the Youjiang Basin, southern China, have been variously correlated to Carlin-style and orogenic gold deposits or classified as a new intermediate deposit type. However, in terms of a multi-scale mineral system approach, they show remarkable similarities to the Tertiary Carlin-type deposits of Nevada and distinct contrasts to orogenic gold deposits. Both the Nevada and Youjiang deposit groups formed in a continent-scale post-orogenic extension event on fragmented continental crust underlain by metasomatized lithosphere. Both form roughly orthogonal deposit trends that subparallel near-orthogonal margins of a continental crustal block, with deposits controlled by gentle anticlines, monoclines or half-horsts and extensional faults, not tight, "locked-up" anticlines, and shear zones. The mineralogy and ore geochemistry of the two groups are similar, with differences consistent with slightly deeper and higher temperature of formation of the older Chinese deposits, commensurate with deeper erosional levels. The Youjiang gold deposits should be classified as Carlin-type, rather than Carlin-like or other terminologies, with their lower gold endowment probably related to a more distal thermal and fluid source than the Nevada Carlin-type deposits.

Introduction

The Youjiang Basin, along the south-eastern margin of the Yangtze Block of southern China (Fig. 1a), hosts numerous gold deposits that collectively have resources of > 800 tonnes (> 25 Moz) gold, with Shuiyindong in the Huijiabao trend contributing about 265 tonnes (7 Moz) gold and Jinfeng in the Lannigou trend contributing 167 tonnes (> 5 Moz) gold (Fig. 1b; Hu et al. 2017a). There has been much controversy concerning their classification and genesis in the Youjiang Basin. Most authors have used the term Carlin-like (Deng and Wang 2016; Stephen et al. 2007) or even Carlin-type (Hu et al. 2002; Pi et al. 2017) to describe them, whereas others have suggested they are intermediate between Carlin-type and orogenic gold deposits (Cline et al. 2013; Xie et al. 2017), or Carlin-style orogenic deposits (Tran et al. 2016), or perhaps simply epizonal orogenic gold deposits (Goldfarb et al. 2018), by analogy to those of the Kuskokwim Basin of southwestern Alaska (Goldfarb et al. 2004). Similarly, there have been correspondingly conflicting suggestions concerning the fluid source, with meteoric, aqueous or organic-rich basin, magmatic, and/or metamorphic fluids all suggested by various authors (Hu et al. 2002, 2017a; Cline et al. 2005), as summarized in Goldfarb et al. (2018).

Although there has been some comparison of the Chinese and Nevada deposits, in terms of tectonic setting, thermal history, and district to deposit-scale structural evolution and geometry, the focus was usually on the intra-deposit scale, such as mineralogical, isotopic and fluid inclusion characteristics of the ore bodies and alteration halos.

Since Wyborn et al. (1994) proposed scale-dependant elements for ore formation, several authors have refined this mineral systems approach, which develops a holistic model across the scales from province, through district to deposit scale to recognize synergies between different mineral-deposit classes (Hronsky et al. 2012; Deng and Wang 2016). Such synergies may have important ramifications in mineral exploration (Groves et al. 2016).

We here adopt a mineral system approach to compare the "Carlin-like" gold deposits of the Youjiang Basin and the

Editorial handling: R. Hu

✉ Qingfei Wang
wqf@cugb.edu.cn

[1] State Key Laboratory of Geological Processes and Mineral Resources, China University of Geosciences, Beijing 100083, China

[2] Centre for Exploration Targeting, University of Western Australia, Nedlands 6009, Australia

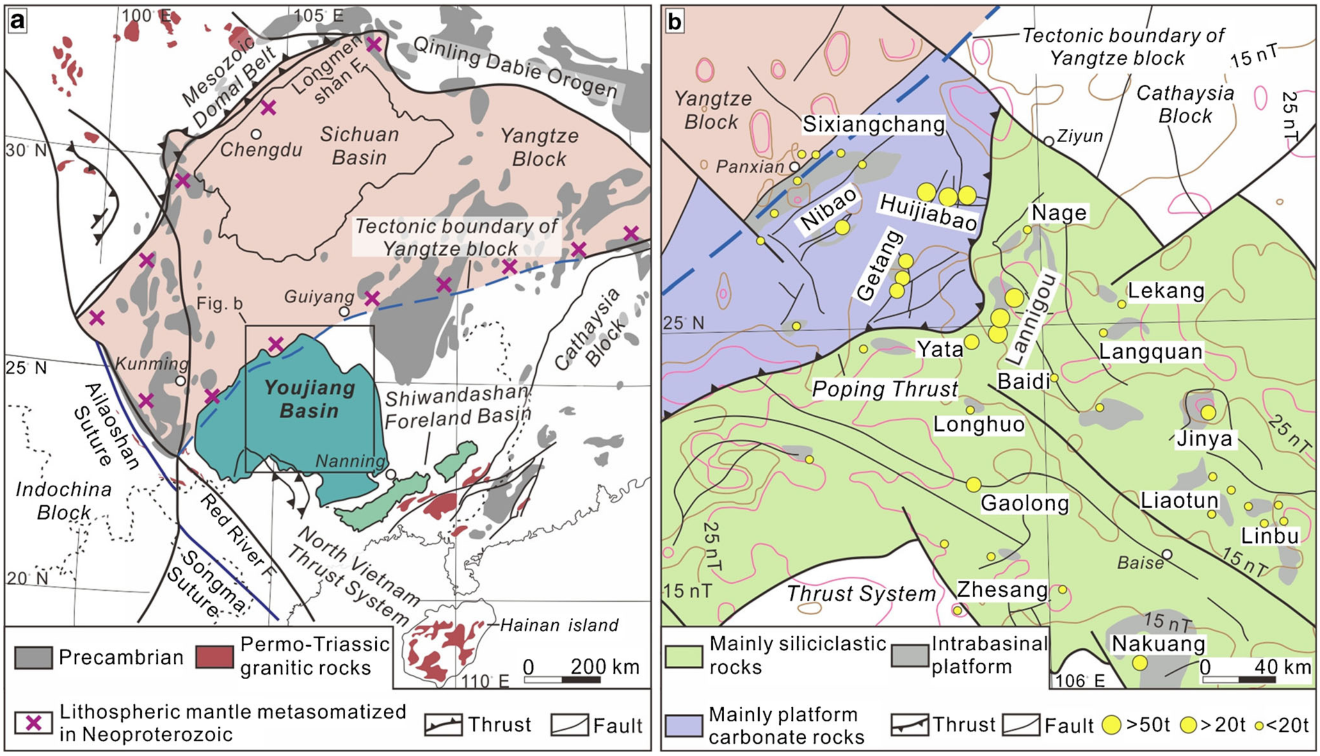

Fig. 1 **a** Simplified geology of the eastern part of the South China Block showing tectonic units discussed in the text. Adapted from Qiao et al. (2015) and Duan et al. (2018); **b** Geology, gold deposits, and aeromagnetic contours (thin light pink and gray lines) in the Youjiang Basin: adapted from Xiong et al. (2013), Peng et al. (2014), Hu et al. (2017b), and Chen et al. (2015b). The Huijabao Trend includes the world-class Shuiyindong deposit as well as the Zimudang and Taopingdong deposits

archetypal Carlin-type gold deposits of Nevada in terms of their key characteristics at different scales. Background information abounds in the published literature and is only summarized here.

Comparisons at the deposit to intra-deposit scale

Deposit geology

Both Nevada Carlin-type and the Youjiang gold deposits comprise a combination of broadly stratabound-replacement and steep brittle fault-controlled mineralization. The Youjiang deposits are hosted both in the platform sequences composed of calcareous and bitumen-bearing rocks and in the basin facies consisting of mudstone and siltstone (Table 1; Gu et al. 2012; Hu et al. 2017a); by contrast, the Nevada deposits are mostly hosted in platform carbonates (Cline 2001; Cline et al. 2013). Both Nevada (Emsbo et al. 2003) and the Youjiang ores (Bao et al. 2005) that are hosted in the platform sequences are associated with bitumen in places.

Equivalent alteration, including silicification, sulfidation, argillization, and decarbonation, are recorded between the majority of Youjiang deposits and the Nevada deposits (Su et al. 2009a; Hou et al. 2016), whereas small differences have been identified in several Youjiang deposits, including the presence of ferroan dolomite, only limited decarbonation, and no low-temperature kaolin (Su et al. 2012; Cline et al. 2013; Xie et al. 2017). Moreover, silicification in the Youjiang deposits produced coarser grained quartz than in the Nevada ores where jasperoid is common as a result of decarbonation (Cline 2001).

Both the Youjiang and Nevada deposits have a similar association of mostly invisible lattice-bound gold in texturally and compositionally zoned pyrite and arsenian pyrite with similar ore-element associations of Au, As, Cu, Hg, Sb, and Tl (Cline 2001; Bao et al. 2005; Cline et al. 2013; Hu et al. 2017a). These broad similarities have led to the widespread classification of the Chinese deposits as Carlin-like. The other arsenic-bearing host minerals for both the Nevada and Youjiang deposits are realgar and orpiment in the late ore stage (Su et al. 2009a; Cline et al. 2013; Hu et al. 2017a). In contrast to the Nevada deposits, the commonly coarser-grained pyrite from the Chinese deposits does not have the consistent arsenic- and gold-rich rims, but economic gold is related to later generations of gold-rich pyrite and arsenopyrite (Su et al. 2012; Hou et al. 2016). Free gold is essentially absent in the Nevada Carlin-type ores but does occur rarely in the Chinese deposits such as at Shuiyindong (Su et al. 2008; Hou et al. 2016).

Table 1 Comparison of gold mineral systems between the Youjiang and Nevada Carlin-type deposits: in order of increasing scale to match discussion in text

Scale	Deposit scale							District scale			Province scale		
Critical features	Alteration	Gold occurrence	Fluid temp.	Fluid pH and salinities	Fluid CO_2	Sulfide $\delta^{34}S$	Fluid $\delta^{18}O$	Structural style	Spatial location	Tectonic regime	Deposit trend	Thermal driver	Metal source
Similar features	Commonly silica sulfide clay carbonate-removal	Lattice-bound in pyrite and arsenical pyrite	Majority in 180 to 240 °C range	pH 4 to 6, 5 to 4 equiv. wt% NaCl	6–8 mol% Youjiang < 4 mol% Nevada	Mostly within 1–10 per mil range	1–17 per mil Youjiang mostly 5–13 per mil with minor negative values Nevada	Stratabound ores in half horsts or gentle anticlines connected to steep fault—controlled ores	Focus around major thrust, mostly in permeable carbonate sequences	Formed after onset of crustal extension	Linear trends subparallel to major bounding faults	Re-activation of metasomatic lithosphere by uprise of astheno-sphere	Uncertain but driven by magmatic-hydrothermal fluids
Youjiang contrast	Dolomite in some deposits	Some visible native gold	60 °C higher in some deposits		Slightly higher CO_2		No negative values reported				Isolated carbonate platform control in places		

In contrast to the Nevada ores, quartz veinlets are common and some contain breccia fragments of the country rocks. These veinlets are sub-vertical and the nature of breccia fragments (Hou et al. 2016) indicates brittle failure. There are no sub-horizontal veins or crack-seal textures to suggest formation via over-pressured fluids (Sibson 2004; Cox 2005) as for most orogenic gold systems (Goldfarb et al. 2005; Yang et al. 2016). A key question is whether the presence of quartz veins marks a significant difference to the Nevada deposits or is because the classic Nevada Carlin-type deposit has underlying dominantly silica-poor dolomites, limestones, and mudstones whereas the Chinese deposits have significant silica-rich turbidite sequences in underlying, or even hosting, stratigraphic successions.

Ore fluids and stable isotopes

Despite the reports of hydrocarbon fluid inclusions in some bitumen-bearing deposits (Gu et al. 2012), the majority of Youjiang gold deposits formed from near-neutral, low-salinity, CH_4-free, and largely aqueous fluids with 6–8 mol% CO_2 at temperatures that locally exceeded 300 °C at depths in excess of 1.7 km and up to 4.3 km (Hu et al. 2002; Cline et al. 2013). As such, they are broadly similar to Carlin-type low-salinity, CH_4-poor ore fluids with < 4 mol% CO_2 at temperatures of 180–240 °C, predominantly at depths between 0.3 and 3.0 km, but possibly as deep as 5 km based on fluid inclusion and geological evidence (Cline and Hofstra 2000). Important differences are the slightly higher CO_2 contents, temperatures, and depths of formation of the Chinese deposits. Only epizonal orogenic gold deposits are formed under similar conditions, but normally from fluids with higher CO_2 contents and commonly with measurable CH_4 (Gebre-Mariam et al. 1995).

Although the $\delta^{34}S$ values of the pyrite from wallrock in the Youjiang deposits range largely from −30 to +30 per mil, those for the Au-bearing pyrite and arsenian pyrite concentrate within 1 to 10 per mil (Table 1; Tan et al. 2015; Hou et al. 2016; Yan et al. 2018). This limited range is interpreted to have resulted from mixing between magmatic fluid and sedimentary material (Hou et al. 2016; Yan et al. 2018). The $\delta^{34}S$ values for Carlin-type ores have a similar range of −1 to +10 per mil (Kesler et al. 2005). The calculated fluid $\delta^{18}O$ values are 1 to 17 per mil for the Chinese deposits (Su et al. 2009a; Peng et al. 2014) and ore-hosting quartz in most Nevada deposits has comparable $\delta^{18}O$ values of −5 to 13 per mil (Emsbo et al. 2003; Cline et al. 2005). The oxygen isotopic compositions of the fluids have commonly been interpreted to represent a deep ore fluid, most likely magmatic-hydrothermal, with varying degrees of water-rock reaction and mixing with meteoric water (Hofstra et al. 1991; Lubben et al. 2012; Tan et al., 2015). No negative $\delta^{18}O$ values were reported in the Youjiang deposits, suggesting limited mixing with meteoric water, perhaps due to their interpreted greater depth of formation. The Youjiang deposits display a wider range in fluid $\delta^{18}O$ values than those of 7 to 13 per mil for Phanerozoic orogenic gold deposits (Goldfarb et al. 2005), possibly due to interaction with contrasting host sequences.

Discussion

The Youjiang and Nevada deposits generally share similar alterations including silicification, argillization, sulfidation, and decarbonation. Sulfidation shows the most consistent relationship to gold mineralization (Cline 2001; Kesler et al. 2003; Ye et al. 2003). The dissolution of ferroan carbonate minerals in the host rocks to provide Fe for sulfidation reactions has been suggested as the most likely precipitation mechanism of gold either as "invisible" or visible gold in arsenian pyrite (Kesler et al. 2003; Su et al. 2008). Given natural intra-group variations at the deposit to intra-deposit scale, the Youjiang deposits have more similarities than contrasts to the Nevada deposits than the orogenic gold deposit (Groves 1993; Goldfarb et al. 2005; Deng et al. 2015; Yang et al. 2016), reinforcing the Carlin-type classification. The main difference is the higher maximum temperature of ~ 60 °C at which the Chinese deposits are interpreted to have formed. This equates to a 1–2 km greater depth of formation, consistent with contrasts in estimated depth ranges. This can potentially explain the coarser-grained auriferous pyrite in the Chinese ores and lesser participation of meteoric water in mixed ore fluids. The approximately 160 Mys difference in mineralization age between the Upper Triassic age of the Chinese deposits (robust Re-Os and Ar-Ar ages listed by Hu et al. (2017a), as discussed further below) and the Eocene age of the Nevada deposits (Cline et al. 2005; Muntean et al. 2011) is also compatible with a different erosional level for the two groups of deposits.

The key question is whether an approximately 60 °C and 1–2 km depth difference mitigates against the classification of the Chinese deposits as Carlin-type, particularly since other mineral deposit classes, such as orogenic gold (Groves 1993), IOCG (Groves et al. 2010), and porphyry copper-gold deposits (Sillitoe and Perelló 2005), can each form a continuum with much greater P-T extremes. This is further examined below at greater scales.

District-scale structural comparisons

Structural histories and geometries

As summarized by Cline et al. (2005) for Nevada deposits and Goldfarb et al. (2018) for the Youjiang deposits, the host terranes for the gold deposits experienced a classic orogenic cycle from compression and transpression to post-orogenic collapse and extension. Early-orogenic thrust and fold structures were both re-activated or overprinted by later extensional structures (Rhys et al. 2015). Although a few authors (Chen et al. 2011, 2015a) suggest that the Chinese deposits formed with a similar timing to the majority of orogenic gold deposits (Goldfarb et al. 2005), at the transition from compression to transpression, the time gap between precise mineralization ages at ca. 210 Ma and initiation of the regional extension at ca. 220 Ma (Wang et al. 2007) support formation of the Youjiang deposits at the onset of extension in the host terranes.

A specific comparison of the structural timing and controls of the gold deposits from Nevada (Rhys et al. 2015) and those of the Youjiang Basin is summarized concisely in Rhys (2017). For Nevada Carlin-type, extension was focused locally on structural highs formed in the earlier compressional deformation phase, with reactivation of existing reverse faults and the development of new extensional faults controlling auriferous fluid ingress to depositional sites (Rhys et al. 2015). Cross-sections of the Nevada deposits commonly illustrate a structural geometry of a combination of stratabound replacement-style orebodies, in gentle monoclines to anticlinal half-horsts, connected to steeply-dipping fault-controlled orebodies (Cline et al. 2005; Rhys et al. 2015; Fig. 2a).

There are similar controls of the Chinese deposits through extensional reactivation of thrusts and folds and generation of an extensional fault system (Figs. 1b and 2b–d; Hu et al. 2017a; Rhys 2017). In places this reactivation was preferentially focused on paleogeographic highs, represented by isolated carbonate platforms that developed from the Early Paleozoic (Su et al. 2009a; Chen et al. 2015b): for example at the Lannigou, Jinya and other deposits (Fig. 1b). The margins of these platforms developed into fault surfaces for selective ore fluid infiltration due to lithological contrasts between platform and surrounding basinal sequences in the extensional setting.

The geometries of ore-controlling structures in the Youjiang Basin are very similar to those in the Nevada district (Table 1). A structural map of the Huijiabao trend, that includes the world-class Shuiyindong deposit, demonstrates well this geometry of a combination of an early anticline with axial-surface parallel reverse (thrust) faults cut by oblique normal faults (Fig. 2b; Hou et al. 2016). Cross-sections of the Taipingdong (Fig. 2b) and Shuiyindong (Fig. 2c) deposits in the Huijiabao trend, and the Lannigou deposit (Fig. 2d), show stratabound gold mineralization sited in gentle anticlines or monoclines, almost identical, if more simplistic, in geometry to cross-sections of the Nevada Carlin-type deposits. Other deposits, such as Yata, consist of steeply dipping orebodies in extensional faults (Zhang et al. 2003).

In the Nevada district, a critical structural component controlling the spatial location of ore deposits the Roberts Mountain Thrust. The thrust juxtaposed siliciclastic and basaltic rocks with the carbonate shelf sequences, the main host

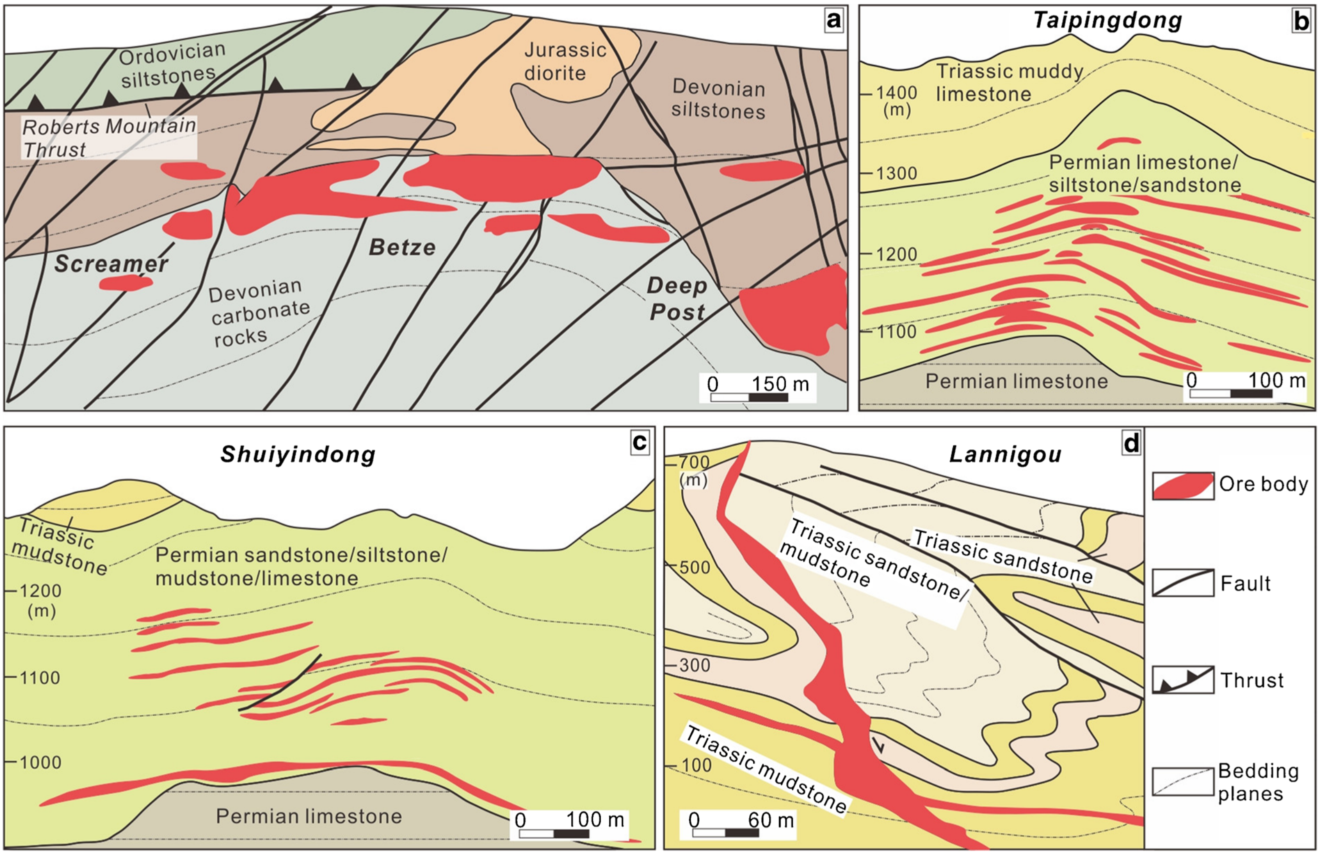

Fig. 2 Cross-sections of characteristics of large gold deposits in the Nevada district and Napanjiang Basin. **a** Screamer-Betze-Deep Post deposits in the Nevada district, from Kesler et al. (2003); **b** Taipingdong deposit in the Huijiabao Trend, from Hou et al. (2016); **c** Shuiyindong deposit in the Huijiabao Trend, from Peng et al. (2014); **d** Lannigou deposit, from Chen et al. 2011

of Carlin-type gold ores (Emsbo et al. 2006). Similarly in the Youjiang basin, the carbonate-dominated units were juxtaposed against siliciclastic rock sequences (Hou et al. 2016; Figs. 1b and 3). The ore deposits in both the Youjiang and Nevada districts are preferentially developed adjacent to the thrust, and the majority of the gold resource, including the world-class Shuiyindong and Jinfeng deposits in the Youjiang Basin, are hosted in the dominantly permeable carbonate units.

Discussion

There are obvious similarities in structural timing, structural regime, and structural geometry between the Youjiang deposits and the Nevada deposits, as also concluded by Rhys et al. (2015), Hu et al. (2017b), and Rhys (2017). These structural geometries are in marked contrast to those of orogenic gold deposits where fold-related deposits are normally sited in tight, reclined, "locked-up" anticlines, and associated thrusts and are typified by sub-horizontal extensional quartz veins (summarized by Groves et al. (2018) and references therein). It must be concluded that the Chinese Carlin-like deposits of the Youjiang Basin meet the criteria for classification as Carlin-type deposits at the district to deposit scale.

Province-scale comparisons

Tectonic setting and geometry of continental crustal margins

The precise tectonic settings of the Nevada province and the Youjiang Basin of China are different. Whereas the Nevada district lies on the fractured margin of the North American Craton which faced the Pacific Ocean throughout its subduction-related compressional to extensional history, the Youjiang Basin is generally considered a foreland basin related to closure of eastern branches of the Paleo-Tethys and subsequent collision between continental blocks (Lehrmann et al. 2007; Deng et al. 2017; Duan et al. 2018). Support for the foreland model is provided by southward thickening of Triassic strata in the Youjiang Basin and the northeast and northwest vergence of folds and thrust faults in northeast Vietnam (Lepvrier et al. 2011) and on the southeastern margin of the Youjiang Basin (Qiao et al. 2015), respectively.

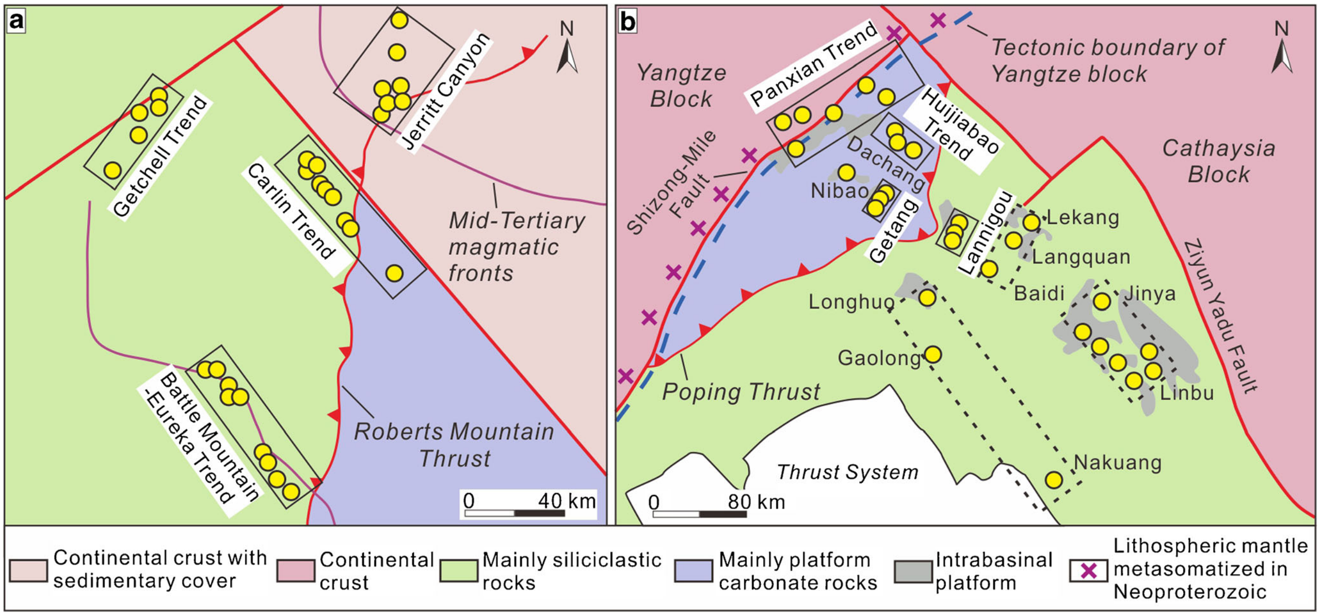

Fig. 3 Schematic maps providing a province-scale comparison between the setting of gold deposits in the Nevada district **a** and in the Youjiang Basin **b**. Features to note include location at near-orthogonal margins of a fragment of continental crust, with gold deposit trends subparallel to these margins, and close spatial association of the gold deposits with a major thrust juxtaposing two parts with contrast lithology. Nevada data derived from, Grauch et al. (2003), Cline et al. (2005), Morrow and Sandberg (2008), Muntean et al. (2011), Watts et al. (2016), and references therein. Youjiang data derived from Stephen et al. (2007), Peng et al. (2014), Chen et al. (2015b), Deng and Wang (2016) and Hou et al. (2016), and references therein

Despite this, the province-scale geometries of the two regions are very similar as are their order-of-magnitude scales. The Nevada district is sited adjacent to a major junction between the regional, broadly NW-SE trending craton margin and a broadly NE-SW trending indentation (Fig. 3a). These almost orthogonal margins, defining the continental crustal block enclosing the majority of the deposits, are defined by Sr and Pb isotope initial ratios and geophysical interpretations (Crafford and Grauch 2002; Grauch et al. 2003). The goldfield trends reflect the near-orthogonal geometry of the continental block margins. The Carlin Trend (approx. 75 km long) and Battle Mountain-Eureka Trend (approx. 125 km long) are subparallel to the regional NW-SE trending craton margin, whereas the Getchell and Jerritt Canyon Trends (approx. 35–40 km long) are subparallel to the NE-SW trending indentation in the craton margin (Fig. 3a).

The northwestern, highly mineralized part of the Youjiang Basin is sited in a continental crustal block bounded by the broadly NE-trending Shizong Mile Fault to the northwest and the broadly NW-SE trending Ziyun Yadu Fault to the northeast (Figs. 1a, 3b). These faults separate the basement rocks of the Yangtze Block from the metasedimentary sequences of the Youjiang Basin, and must have been two of the fundamental crustal to lithospheric faults that controlled both the evolution and gold distribution of the basin (Hu et al. 2017a and references therein). As in the Nevada district, the goldfields define roughly orthogonal trends that subparallel the fault boundaries (Figs. 3a, b). The Huijiabao Trend (approx. 40 km long), that includes the world-class Shuiyindong deposit, as well as the Zimudang and Taopingdong deposits, trend broadly WNW-ESE subparallel to the Ziyun Yadu Fault, whereas the Getang Trend (approx. 30 km long) and Lannigou Trend (approx. 30 km long), that includes the world-class Jinfeng deposit, as well as the Panxian trend along the northewestern boundary of Youjiang Basin are subparallel to the NE-SW trending Shizong Mile Fault. Other gold trends are less well-defined and are shown as less-robust trends in Fig. 3b based on the trends of sporadic individual deposits. The definition of such trends has obvious exploration implications for the distribution of as-yet-undiscovered deposits.

Thermal drivers for gold mineralization

Although the precise tectonic processes for generation of a regional-scale thermal anomaly responsible for gold mineralization over tens of thousands of square kilometers at both the Nevada and Youjiang districts are debated, the thermal drivers appear broadly similar.

In the Nevada district, possibly through the removal of the Fallon subduction slab (Cline et al. 2005), onset of extension and uprise of asthenosphere resulted in melting of previously metasomatized lithosphere to produce basic to ultrabasic melts that ponded at the MOHO and melted continental crust. This led to intrusion of a series of hybrid high-K granitic melts which are considered to be the heat and probable ultimate fluid sources for the Nevada deposits, as summarized by Cline et al. (2005) and Muntean et al. (2011). Despite the recognition of a few Eocene syn-gold intrusions exposed in the Nevada district (Maroun et al. 2017), their spatial relationship to the Nevada gold deposits is largely inferred from geophysical data (Ressel and Henry 2006). The evolution from the inferred high-T magmatic hydrothermal ore fluids to the low-T fluids that deposited the gold and the depositional mechanisms themselves are still controversial (Cline et al. 2005; Muntean et al. 2011). Continued extension resulted in the development of a series of metamorphic core complexes extending for over 1000 km along the eastern margin of the Nevada province, characterized by the Basin-and-Range terrain (Konstantinou et al. 2013), with the slightly off-trend Ruby Mountains metamorphic complex being the most proximal to the Carlin Trend (Howard 2003).

The thermal driver for the evolution of the Youjiang goldfields has been unclear as there are no recorded granitic intrusions coeval with the gold mineralization in the basin (Zhu et al. 2017), one of the major factors in the controversy concerning the classification of the Chinese deposits. Any heat or fluid source is constrained by the age of gold mineralization. The recent robust ages include ca. 223–185 Ma from Ar/Ar of sericite and Re-Os of arsenopyrite for Jinfeng (Chen et al. 2015a); ca. 218–209 Ma for Zhesang from Ar/Ar in sericite and U-Pb in rutile (Pi et al. 2016, 2017); ca. 218–209 Ma for Laozhaiwan from U-Pb in monazite (Hu et al. 2017a); and 268 (240)-202 Ma for Shuiyindong (Chen et al. 2015a). Collectively, these data suggest that gold mineralization took place in the Upper Triassic at ca. 210 Ma. Samarium-Nd isochron ages of 134 to 136 Ma reported for hydrothermal calcite from the Shuiyingdong deposit (Su et al. 2009b), probably represent a later limited hydrothermal overprint.

It is thus instructive to examine what thermal events were occurring in the vicinity of the Youjiang Basin during the mineralization period. In the Upper Triassic, there was also a post-collisional extensional event along the Ailaoshan-Songma Paleotethyan Suture on the western margin of the Yangtze Block. This is manifested by the development of extensional basins and basic-felsic magmatism (Yang et al. 2018; Fig. 1a). South of the Youjiang Basin, this critical period was also characterized by extension, after Early to Middle Triassic intraplate crustal shortening with folding and associated thrusting in North Vietnam and the Shiwandashan basin (Lepvrier et al. 2011; Wang et al. 2007). On the north-western margin of the Yangtze Block, a > 1000-km long Mesozoic domal belt associated with synchronous granite intrusion (Fig. 1a) has been interpreted to be related to asthenosphere upwelling and consequent crustal extension (Roger et al. 2004; Sigoyer et al. 2014). However, as discussed above, there is no direct evidence of magmatism in the Youjiang Basin at this time.

Discussion

Although their tectonic settings are different, both the Nevada and Youjiang gold districts formed during post-orogenic extension adjacent to crustal- to lithosphere-scale faults bounding the margins of continental crustal blocks. They are both sited in anomalous geometrical configurations on these fragment margins where first-order faults are locally orthogonal (Fig. 3). The linear trends of the goldfields and gold deposits in both cases are subparallel to the bounding faults, with individual trends almost orthogonal to each other, although the Nevada trends are more extensive, commensurate with their far greater gold endowment.

Formation of the Nevada Carlin-type deposits was driven by asthenosphere uprise that acted as a thermal anomaly (Muntean et al. 2011) to instigate the uprise of metamorphic core complexes and melt both metasomatized lithosphere and crust to produce hybrid magmas that were intruded as granitic plutons into the sedimentary rocks of the continental margin (Cline et al. 2005). The Carlin-type ores are interpreted to be deposited from a highly modified magmatic-hydrothermal fluid that was exsolved from these plutons.

There are no recorded granitic intrusions within the Youjiang Basin despite the clear evidence for extensional tectonics at the time of gold mineralization. This does not necessarily mean that no granitic plutons were intruded as the magmatic association in the Nevada district was only recognized initially from high-quality company-generated aeromagnetic surveys (Ressel and Henry 2006), and only later confirmed from rare outcrops of gold-synchronous granites (Muntean et al., 2011). In the Youjiang Basin, there are positive aeromagnetic anomalies spatially related to the ore districts (Xiong et al. 2013; Fig. 1b), but it is currently unclear if these relate to concealed intrusions of appropriate age to be gold-related. The specific trending of the Youjiang gold deposits parallel to the margins of a continental block and the extensional timing of gold mineralization in that block are in direct contrast to the tectonic settings and transpressional timing of the majority of orogenic gold deposits.

An important similarity between the Nevada and Youjiang gold districts is the presence of metasomatized lithosphere beneath the continental crust (Muntean et al. 2011; Zhao et al. 2011). The south-eastern margin of the Yangtze Block has witnessed an episode of oceanic subduction in the Neoproterozoic resulting in such metasomatism (Zhao et al. 2011), and the world-class Huijiabao and Lannigou deposits are above similarly modified lithosphere along the south-eastern boundary of the Yangtze Block (Fig. 1a). However, unless it can be shown that melting of such metasomatized lithosphere produced intrusions coeval with gold mineralization, the possibility that the Youjiang gold deposits had a more distal thermal energy and fluid source than the Nevada deposits must be considered. Such a model has the potential to explain their order-of-magnitude lower gold endowment.

Conclusions

An across-scales comparison between the Triassic, largely carbonate-hosted, gold deposits of the Triassic Youjiang Basin and the Tertiary Nevada deposits is instructive. At the deposit to intra-deposit scale, there are numerous similarities to the Tertiary Nevada deposits, with differences that can be explained by formation of the older Youjiang deposits at up to 60 °C higher temperatures and up to 2 km greater depths commensurate with deeper erosion levels: a difference well within the limits of variation of other coherent gold-deposit classes. At the district to deposit scale, the Nevada and Youjiang deposits are both characteristically sited in gentle anticlines, monoclines, and/or half-horsts or along extensional faults in previously-deformed sedimentary sequences. At the province scale, both the Nevada and Youjiang gold deposits form sets of almost orthogonal trends that are subparallel to the margins of continental crustal blocks underlain by metasomatized lithosphere. An apparent more proximal source of thermal energy and deep fluid in the Nevada district can best explain its order-of-magnitude greater gold resource in the current absence of definitive evidence for intrusion of syn-gold hybrid magmas into the Youjiang Basin. It can be concluded that the Chinese deposits are comparable with the Nevada deposits within a mineral system context and should be classified as Carlin-type deposits.

Acknowledgements The constructive review from Profs Bernd Lehmann and Ruizhong Hu is greatly appreciated. We are grateful to Rich Goldfarb for access to his paper in press on Chinese gold deposits. David Groves is grateful to Jun Deng and Liqiang Yang for their support which has allowed him to collaborate in CUGB-based research.

Funding information This research was jointly supported by the National Key Research and Development Project of China (2016YFC0600307), and the National Key Basic Research Development Program (973 Program; 2015CB452606).

References

Bao Z, Zhao Z, Guham J (2005) Organic geochemistry of sedimentary rock-hosted disseminated gold deposits in southwestern Guizhou Province, China. Acta Geol Sin 79:120–133

Chen MH, Mao JW, Bierlein FP, Norman T, Uttley PJ (2011) Structural features and metallogenesis of the Carlin-type Jinfeng (Lannigou) gold deposit, Guizhou Province, China. Ore Geol Rev 43:217–234

Chen MH, Mao JW, Li C, Zhang ZQ, Dang Y (2015a) Re-Os isochron ages for arsenopyrite from Carlin-like gold deposits in the Yunnan-Guizhou-Guangxi “golden triangle”, southwestern China. Ore Geol Rev 64:316–327

Chen MH, Zhang Z, Santosh M, Dang Y, Zhang W (2015b) The Carlin-type gold deposits of the “golden triangle” of SW China: Pb and S isotopic constraints for the ore genesis. J Asian Earth Sci 103:115–128

Cline JS (2001) Timing of gold and arsenic sulfide mineral deposition at the Getchell Carlin-type gold deposit, north-central Nevada. Econ Geol 96:75–89

Cline JS, Hofstra AA (2000) Ore-fluid evolution at the Getchell Carlin-type gold deposit, Nevada, USA. Eur J Mineral 12:195–212

Cline JS, Hofstra AH, Muntean JL, Tosdal RM, Hickey KA (2005) Carlin-type gold deposits in Nevada: critical geologic characteristics and viable models. Econ Geol 100th Anniv Volume:451–484

Cline JS, Muntean JL, Gu XX, Xia Y (2013) A comparison of Carlin-type gold deposits: Guizhou Province, golden triangle, Southwest China, and northern Nevada, USA. Front Earth Sci-Proc 20:1–18

Cox SF (2005) Coupling between deformation, fluid pressures, and fluid flow in ore-producing hydrothermal systems at depth in the crust. Econ Geol 100th Anniv Volume:39–75

Crafford AEJ, Grauch VJS (2002) Geologic and geophysical evidence for the influence of deep crustal structures on Paleozoic tectonics and the alignment of world-class gold deposits, north-central Nevada, USA. Ore Geol Rev 21:157–184

Deng J, Wang C, Bagas L, Carranza EJM, Lu Y (2015) Cretaceous–Cenozoic tectonic history of the Jiaojia Fault and gold mineralization in the Jiaodong Peninsula, China: constraints from zircon U–Pb, illite K–Ar, and apatite fission track thermochronometry. Mineral Deposita 50:987–1006

Deng J, Wang QF (2016) Gold mineralization in China: Metallogenic provinces, deposit types and tectonic framework. Gondwana Res 36:219–274

Deng J, Wang QF, Li GJ (2017) Tectonic evolution, superimposed orogeny, and composite metallogenic system in China. Gondwana Res 50:216–266

Duan L, Meng QR, Christie-Blick N, Wu GL (2018) New insights on the Triassic tectonic development of South China from the detrital zircon provenance of Nanpanjiang turbidites. GSA Bull 130:24–34

Emsbo P, Groves DL, Hofstra AH, Bierlein FP (2006) The giant Carlin gold province: a protracted interplay of orogenic, basinal and hydrothermal processes above a lithospheric boundary. Mineral Deposita 41:517–525

Emsbo P, Hofstra AH, Lauha EA, Griffin GL, Hutchinson RW (2003) Origin of high-grade gold ore, source of ore fluid components, and genesis of the Meikle and neighboring Carlin-type deposits, northern Carlin Trend, Nevada. Econ Geol 98:1069–1105

Gebre-Mariam M, Hagemann SG, Groves DI (1995) A classification scheme for epigenetic Archaean lode-gold deposits. Mineral Deposita 30:408–410

Goldfarb RJ, Ayuso R, Miller ML (2004) The Late Cretaceous Donlin Creek deposit, southwestern Alaska – controls on epizonal formation. Econ Geol 99:643–671

Goldfarb RJ, Baker T, Dubé D, Groves DI, Hart CJR, Gosselin P (2005) Distribution, character, and genesis of gold deposits in metamorphic terranes. Econ Geol 100th Anniv Volume:407–450

Goldfarb RJ, Qiu KF, Deng J, Chen YJ, Yang LQ (2018) Orogenic gold deposits of China. In: Goldfarb RJ, Chang ZS (eds) Deposit in China. SEG Special Publications (In press)

Grauch VJS, Rodriguez BD, Wooden JL (2003) Geophysical and isotopic constraints on crustal structure related to mineral trends in north-Central Nevada and implications for tectonic history. Econ Geol 98:269–286

Groves DI (1993) The crustal continuum model for late-Archaean lode-gold deposits of the Yilgarn Block, Western Australia. Mineral Deposita 28:366–374

Groves DI, Bierlein FP, Meinert LA, Hitzman MW (2010) Iron-oxide copper-gold (IOCG) deposits through Earth history: implications for origin, lithospheric setting and distinction from other epigenetic iron oxide deposits. Econ Geol 105:641–654

Groves DI, Goldfarb RJ, Santosh M (2016) The conjunction of factors that lead to formation of giant gold provinces and deposits in non-arc settings. Geosci Front 7:303–314

Groves DI, Santosh M, Goldfarb RJ, Zhang L (2018) Structural geometry of orogenic gold deposits: implications for exploration of world-class and giant deposits. Geosci Front 9:1163–1177. https://doi.org/10.1016/j.gsf.2018.01.006

Gu XX, Zhang YM, Li BH, Dong SY, Xue CJ, Fu SH (2012) Hydrocarbon-and ore-bearing basinal fluids: a possible link between gold mineralization and hydrocarbon accumulation in the Youjiang basin, South China. Mineral Deposita 47:663–682

Hofstra AH, Leventhal JS, Northrop HR, Landis GP, Rye RO, Birak DJ, Dahl AR (1991) Genesis of sediment-hosted disseminated-gold deposits by fluid mixing and sulfidization: chemical-reaction-path modeling of ore-depositional processes documented in the Jerritt Canyon district, Nevada. Geology 19:36–40

Hou L, Peng HJ, Ding J, Zhang JR, Zhu SB, Wu SY, Wu Y, Ouyang HG (2016) Textures and in situ chemical and isotopic analyses of pyrite, Huijiabao Trend, Youjiang basin, China: implications for paragenesis and source of sulfur. Econ Geol 111:331–353

Howard KA (2003) Crustal structure of the Elko-Carlin region, Nevada, during Eocene gold mineralization: Ruby Mountains-East Humboldt metamorphic core complex as a guide to the deep crust. Econ Geol 98:249–268

Hronsky JMA, Groves DI, Loucks RR, Begg GC (2012) A unified model for gold mineralisation in accretionary orogens and implications for regional-scale exploration targeting methods. Mineral Deposita 47: 339–358

Hu RZ, Su WC, Bi XW, Tu GZ, Hofstra AH (2002) Geology and geochemistry of Carlin-type gold deposits in China. Mineral Deposita 37:378–392

Hu RZ, Fu SL, Huang Y, Zhou MF, Fu SH, Zhao CH, Wang YJ, Bi XW, Xiao JF (2017a) The giant South China Mesozoic low-temperature metallogenic domain: reviews and a new geodynamic model. J Asian Earth Sci 137:9–34

Hu Y, Liu W, Wang J, Zhang G, Zhou Z, Han R (2017b) Basin-scale structure control of Carlin-style gold deposits in central southwestern Guizhou, China: insights from seismic reflection profiles and gravity data. Ore Geol Rev 91:444–462

Kesler SE, Fortuna J, Ye Z, Alt JC, Core DP, Zohar P, Borhauer J, Chryssoulis SL (2003) Evaluation of the role of sulfidation in deposition of gold, screamer section of the Betze-Post Carlin-type deposit, Nevada. Econ Geol 98:1137–1157

Kesler SE, Riciputi LC, Ye Z (2005) Evidence for a magmatic origin for Carlin-type gold deposits: isotopic composition of sulfur in the Betze-Post-Screamer Deposit, Nevada, USA. Mineral Deposita 40: 127–136

Konstantinou A, Strickland A, Miller E, Valley JW (2013) Syn-extensional magmatism leading to crustal flow in the Albion-Raft-River creek metamorphic core complex, northeastern basin and range. Tectonics 32:1384–1403

Lehrmann DJ, Pei D, Enos P, Minzoni M, Ellwood BB, Orchard MJ, Zhang JY, Wei JY, Dillett P, Koenig J, Steffen K, Druke D, Druke J, Kessel B, Newkirk T (2007) Impact of differential tectonic subsidence on isolated carbonate-platform evolution: Triassic of the Nanpanjiang Basin, South China. AAPG Bull 91:287–320

Lepvrier C, Faure M, Van VN, Vu TV, Lin W, Trong TT, Hoa PT (2011) North-directed Triassic nappes in northeastern Vietnam (East Bac Bo). J Asian Earth Sci 41:56–68

Lubben JD, Cline JS, Barker SL (2012) Ore fluid properties and sources from quartz-associated gold at the Betze-Post Carlin-type gold deposit, Nevada, United States. Econ Geol 107:1351–1385

Maroun LRC, Cline JS, Simon A, Anderson P, Muntean J (2017) High-grade gold deposition and collapse breccia formation, Cortez Hills Carlin-type gold deposit, Nevada, USA. Econ Geol 112:707–740

Morrow JR, Sandberg CA (2008) Evolution of Devonian carbonate-shelf margin, Nevada. Geosphere 4:445–458

Muntean JL, Cline JS, Simon AC, Longo AA (2011) Magmatic hydrothermal origin of Nevada's Carlin-type gold deposits. Nat Geosci 4: 122–127

Peng YW, Gu XX, Zhang YM, Liu L, Wu CY, Chen SY (2014) Ore-forming process of the Huijiabao gold district, southwestern Guizhou Province, China: evidence from fluid inclusions and stable isotopes. J Asian Earth Sci 93:89–101

Pi QH, Hu RZ, Peng KQ, Wu JB, Wei ZW, Huang Y (2016) Geochronology of the Zhesang gold deposit and mafic rock in Funing County of Yunnan Province, with special reference to the dynamic background of Carlin-type gold deposits in the Dian-Qian-Gui region. Acta Petrol Sin 32:3331–3342 (in Chinese)

Pi QH, Hu RZ, Xiong B, Li QL, Zhong RC (2017) In situ SIMS U-Pb dating of hydrothermal rutile: reliable age for the Zhesang Carlin-type gold deposit in the golden triangle region, SW China. Mineral Deposita 52:1179–1190

Qiao L, Wang QF, Li C (2015) The western segment of the suture between the Yangtze and Cathaysia blocks: constraints from inherited and co-magmatic zircons from Permian S-type granitoids in Guangxi, South China. Terra Nova 27:392–398

Ressel MW, Henry CD (2006) Igneous geology of the Carlin trend, Nevada: development of the Eocene plutonic complex and significance for Carlin-type gold deposits. Econ Geol 101:347–383

Rhys D (2017) Advances in the understanding of the structural controls on Carlin deposits in Nevada: implications for Chinese Carlin-like systems [ext. abs.]: SEG: ore deposits of Asia: China and beyond, 88th, Bejing, China, Extended Abstracts, 468–471

Rhys D, Valli F, Burgess R, Heitt D, Griesel G, Hart K (2015) Controls of fault and fold geometry on the distribution of gold mineralization on the Carlin trend. In: New Concepts and Discoveries, Geol Soc Nev Symp. DEStech Publications, Inc, pp 333–389

Roger F, Malavieille J, Leloup PH, Calassou S, Xu ZQ (2004) Timing of granite emplacement and cooling in the Songpan Garzê fold belt (eastern Tibetan plateau) with tectonic implications. J Asian Earth Sci 22:465–481

Sibson RH (2004) Controls on maximum fluid overpressure defining conditions for mesozonal mineralization. J Struct Geol 26:1127–1136

Sigoyer JD, Vanderhaeghe O, Duchêne S, Billerot A (2014) Generation and emplacement of Triassic granitoids within the Songpan Ganze accretionary-orogenic wedge in a context of slab retreat accommodated by tear faulting, eastern Tibetan plateau, China. J Asian Earth Sci 88:192–216

Sillitoe RH, Perelló J (2005) Andean copper province: tectono-magmatic settings, deposit types, metallogeny, exploration, and discovery. Econ Geol 100th Anniv Volume:845–890

Stephen GP, Huang JZ, Li ZP, Jing CG (2007) Sedimentary rock-hosted Au deposits of the Dian-Qian-Gui area, Guizhou, and Yunnan Provinces, and Guangxi District, China. Ore Geol Rev 31:170–204

Su WC, Xia B, Zhang HT, Zhang XC, Hu RZ (2008) Visible gold in arsenian pyrite at the Shuiyindong Carlin-type gold deposit, Guizhou, China: implications for the environment and processes of ore formation. Ore Geol Rev 33:667–679

Su WC, Heinrich CA, Pettke T, Zhang X, Hu R, Xia B (2009a) Sediment-hosted gold deposits in Guizhou, China: products of wall-rock sulfidation by deep crustal fluids. Econ Geol 104:73–93

Su WC, Hu RZ, Xia B, Xia Y, Liu Y (2009b) Calcite Sm-Nd isochron age of the Shuiyindong Carlin-type gold deposit, Guizhou, China. Chem Geol 258:269–274

Su WC, Zhang H, Hu R, Ge X, Xia B, Chen Y, Zhu C (2012) Mineralogy and geochemistry of gold-bearing arsenian pyrite from the Shuiyindong Carlin-type gold deposit, Guizhou, China: implications for gold depositional processes. Mineral Deposita 47:653–662

Tan QP, Xia Y, Xie ZJ, Yan J, Wei D (2015) S, C, O, H, and Pb isotopic studies for the Shuiyindong Carlin-type gold deposit, Southwest Guizhou, China: constraints for ore genesis. Chinese J Geophys-Ch 34:525–539

Tran TH, Nevolko PA, Ngo TP, Svetlitskaya TV, Vu HL, Redin Y, Tran TA, Pham TD, Ngo TH (2016) Geology, geochemistry and sulphur isotopes of the Hat Han gold-antimony deposit, NE Vietnam. Ore Geol Rev 78:69–84

Wang Y, Fan W, Cawood PA, Ji SH, Peng T, Chen X (2007) Indosinian high-strain deformation for the Yunkaidashan tectonic belt, South China: kinematics and $^{40}Ar/^{39}Ar$ geochronological constraints. Tectonics 26

Watts KE, John DA, Colgan JP, Henry CD, Bindeman IN, Schmitt AK (2016) Probing the volcanic–plutonic connection and the genesis of crystal-rich rhyolite in a deeply dissected supervolcano in the Nevada Great Basin: source of the late Eocene Caetano tuff. J Petrol 57:1599–1644

Wyborn LAI, Heinrich CA, Jaques AL (1994) Australian Proterozoic mineral systems: essential ingredients and mappable criteria. In: The AusIMM Annual Conference, vol 1994, pp 109–115 (Darwin: AusIMM)

Xie ZJ, Xia Y, Cline JS, Yan BW, Wang ZP (2017) Comparison of the native antimony-bearing Paiting gold deposit, Guizhou Province, China, with Carlin-type gold deposits, Nevada, USA. Mineral Deposita 52:69–84

Xiong SQ, Fan ZG, Zhang HR, Huang XZ, Ding YY, Li ZK, Zhou DQ (2013) Series aeromagnetic map of China mainland (1:5,000,000) and its instructions. China Geological Publishing House, Beijing (in Chinese)

Yan J, Hu R, Liu S, Lin Y, Zhang J, Fu S (2018) NanoSIMS element mapping and sulfur isotope analysis of Au-bearing pyrite from Lannigou Carlin-type Au deposit in SW China: new insights into the origin and evolution of Au-bearing fluids. Ore Geol Rev 92:29–41

Yang LQ, Deng J, Wang ZL, Guo LN, Li RH, Groves DI, Danyushevsky LV, Zhang C, Zhao H (2016) Relationships between gold and pyrite at the Xincheng gold deposit, Jiaodong Peninsula, China: implications for gold source and deposition in a brittle epizonal environment. Econ Geol 111:105–126

Yang L, Wang QF, Wang YN, Li GJ (2018) Proto- to Paleo-Tethyan evolution of the eastern margin of Simao block. Gondwana Res doi 62:61–74. https://doi.org/10.1016/j.gr.2018.02.012

Ye ZJ, Kesler SE, Essene EJ, Zohar PB, Borhauer JL (2003) Relation of Carlin-type gold mineralization to lithology, structure and alteration: screamer zone, Betze-Post deposit. Nevada Miner Deposita 38:22–38

Zhao JH, Zhou MF, Yan DP, Zheng JP, Li JW (2011) Reappraisal of the ages of Neoproterozoic strata in South China: no connection with the Grenvillian orogeny. Geology 39:299–302

Zhang XC, Spiro B, Halls C (2003) Sediment-hosted disseminated gold deposits in Southwest Guizhou, PRC: their geological setting and origin in relation to mineralogical, fluid inclusion, and stable-isotope characteristics. Int Geol Rev 45:407–470

Zhu JJ, Hu RZ, Richards JP, Bi XW, Stern R, Lu G (2017) No genetic link between Late Cretaceous felsic dikes and Carlin-type Au deposits in the Youjiang basin, Southwest China. Ore Geol Rev 84:328–337